

Luminescent Ruthenium(II)– and Rhenium(I)–Diimine Wires Bind Nitric Oxide Synthase

Alexander R. Dunn,[†] Wendy Belliston-Bittner,[†] Jay R. Winkler,[†]
Elizabeth D. Getzoff,[‡] Dennis J. Stuehr,[§] and Harry B. Gray^{*†}

Contribution from the Beckman Institute, California Institute of Technology, Pasadena, California 91125, Department of Molecular Biology and Skaggs Institute for Chemical Biology, The Scripps Research Institute, MS MB4, 10550 North Torrey Pines Road, La Jolla, California 92037, and Department of Immunology, Lerner Research Institute, The Cleveland Clinic, Cleveland, Ohio 44195

Received May 22, 2004; Revised Manuscript Received January 27, 2005; E-mail: hbgray@caltech.edu

Abstract: Ru(II)– and Re(I)–diimine wires bind to the oxygenase domain of inducible nitric oxide synthase (iNOS_{oxy}). In the ruthenium wires, [Ru(L)₂L']²⁺, L' is a perfluorinated biphenyl bridge connecting 4,4'-dimethylbipyridine to a bulky hydrophobic group (adamantane, **1**), a heme ligand (imidazole, **2**), or F (**3**). **2** binds in the active site of the murine iNOS_{oxy} truncation mutants Δ65 and Δ114, as demonstrated by a shift in the heme Soret from 422 to 426 nm. **1** and **3** also bind Δ65 and Δ114, as evidenced by biphasic luminescence decay kinetics. However, the heme absorption spectrum is not altered in the presence of **1** or **3**, and Ru–wire binding is not affected by the presence of tetrahydrobiopterin or arginine. These data suggest that **1** and **3** may instead bind to the distal side of the enzyme at the hydrophobic surface patch thought to interact with the NOS reductase module. Complexes with properties similar to those of the Ru–diimine wires may provide an effective means of NOS inhibition by preventing electron transfer from the reductase module to the oxygenase domain. Rhenium–diimine wires, [Re(CO)₃L₁L'₁]⁺, where L₁ is 4,7-dimethylphenanthroline and L'₁ is a perfluorinated biphenyl bridge connecting a rhenium-ligated imidazole to a distal imidazole (F₈bp-im) (**4**) or F (F₉bp) (**5**), also form complexes with Δ114. Binding of **4** shifts the Δ114 heme Soret to 426 nm, demonstrating that the terminal imidazole ligates the heme iron. Steady-state luminescence measurements establish that the 4:Δ114 dissociation constant is 100 ± 80 nM. Re–wire **5** binds Δ114 with a K_d of 5 ± 2 μM, causing partial displacement of water from the heme iron. Our finding that both **4** and **5** bind in the NOS active site suggests novel designs for NOS inhibitors. Importantly, we have demonstrated the power of time-resolved FET measurements in the characterization of small molecule:protein interactions that otherwise would be difficult to observe.

Introduction

The enzyme nitric oxide synthase (NOS) is the major biological source of nitric oxide (NO), a secondary messenger acting in a myriad of circumstances that include neuronal development, regulation of blood pressure, apoptosis, neurotransmission, and immunological response.^{1–7} Because of the central importance of NO, NOS has been implicated in septic shock, inflammation, a variety of neurodegenerative disorders, and heart disease.^{8–10}

Full-length NOS consists of oxygenase, reductase, and calmodulin binding domains. The NOS oxygenase domain (NOS_{oxy}), which contains cysteine-ligated heme and tetrahydrobiopterin (H₄B) cofactors, catalyzes the conversion of arginine and molecular oxygen to NO and citrulline.¹¹ The electrons necessary for this reaction are provided by the reductase module, which is attached to NOS_{oxy} by a calmodulin-binding linker.^{12,13} NOS functions as a homodimer; the reductase module from one half of the dimer reduces the oxygenase domain of the other.^{14,15} Calmodulin binding is

[†] California Institute of Technology.

[‡] The Scripps Research Institute.

[§] The Cleveland Clinic.

- (1) Kendrick, K. M.; Guevara-Guzman, R.; Zorrilla, J.; Hinton, M. R.; Broad, K. D.; Mimmack, M.; Ohkura, S. *Nature* **1997**, *388*, 670–674.
- (2) Huang, P. L.; Huang, Z. H.; Mashimo, H.; Bloch, K. D.; Moskowitz, M. A.; Bevan, J. A.; Fishman, M. C. *Nature* **1995**, *377*, 239–242.
- (3) Ko, G. Y.; Kelly, P. T. *J. Neurosci.* **1999**, *19*, 6784–6794.
- (4) Luth, H. J.; Holzer, M.; Gertz, H. J.; Arendt, T. *Brain Res.* **2000**, *852*, 45–55.
- (5) Mize, R. R.; Dawson, T. M.; Dawson, V. L.; Friedlander, M. J. *Nitric Oxide in Brain Development, Plasticity and Disease*; Elsevier: Amsterdam, 1998.
- (6) Nathan, C. *J. Clin. Invest.* **1997**, *100*, 2417–2423.
- (7) Lancaster, J. *Nitric Oxide: Principles and Actions*; Academic Press: San Diego, CA, 1996.

- (8) Hobbs, A. J.; Higgs, A.; Moncada, S. *Annu. Rev. Pharmacol. Toxicol.* **1999**, *39*, 191–220.
- (9) Heales, S. J. R.; Bolaños, J. P.; Stewart, V. C.; Brookes, P. S.; Land, J. M.; Clark, J. B. *Biochim. Biophys. Acta* **1999**, *1410*, 215–228.
- (10) Hingorani, A. D.; Liang, C. F.; Fatibene, J.; Lyon, A.; Monteith, S.; Parsons, A.; Haydock, S.; Hopper, R. V.; Stephens, N. G.; O'Shaughnessy, K. M.; Brown, M. J. *Circulation* **1999**, *100*, 1515–1520.
- (11) Stuehr, D. J. *Biochim. Biophys. Acta* **1999**, *1411*, 217–230.
- (12) Cho, H. J.; Xie, Q. W.; Calaycay, J.; Mumford, R. A.; Swiderek, K. M.; Lee, T. D.; Nathan, C. *J. Exp. Med.* **1992**, *176*, 599–604.
- (13) Bredt, D. S.; Hwang, P. M.; Glatt, C. E.; Lowenstein, C.; Reed, R. R.; Snyder, S. H. *Nature* **1991**, *351*, 714–718.
- (14) Crane, B. R.; Rosenfeld, R. J.; Arvai, A. S.; Ghosh, D. K.; Ghosh, S.; Tainer, J. A.; Stuehr, D. J.; Getzoff, E. D. *EMBO J.* **1999**, *18*, 6271–6281.

known to modulate electron transfer and, hence, catalysis.^{16–18} Several crystal structures of the NOS oxygenase domain have been determined,^{19–21} but the structure of the full-length enzyme remains elusive.

We have a long-standing interest in the high-valent intermediates thought to play key roles in heme-mediated oxidations.^{22–29} To observe these intermediates, we have designed Ru–diimine photosensitizers (Ru–wires) that bind to the mechanistically related enzyme cytochrome P450 and inject an electron into the active site upon excitation with 470-nm light.²⁷ Energy transfer between the excited state of the Ru–wire and the heme also serves as a sensitive structural probe.^{22,29} Like NOSoxy, cytochrome P450 enzymes possess a cysteine-ligated heme in the active site and catalyze the oxidation of substrates using molecular oxygen and two electrons supplied by a reductase (in the case of P450, a separate protein).³⁰

Given the postulated mechanistic similarities between NOS and cytochrome P450, we have endeavored to develop similar photosensitizer–wires for NOS. Our initial investigation showed that complexes **1–3** bind the oxygenase domain of murine inducible NOS (iNOSoxy) with micromolar dissociation constants. Intriguingly, a combination of fluorescence energy transfer (FET) measurements and structural modeling suggests that **1** and **3** bind to the surface patch thought to interact with the reductase module. Second generation compounds **4** and **5**, which are structurally analogous to **2** and **3**, bind in the iNOSoxy active site with micro- and nanomolar dissociation constants.

Experimental Section

Murine inducible NOS oxygenase domain constructs with N-terminal truncations at residues 65 ($\Delta 65$) and 114 ($\Delta 114$) were prepared as previously described.³¹ Small aliquots of the protein solutions were exchanged into phosphate buffer (50 mM potassium phosphate, 100 mM potassium chloride, pH 7.2) using a desalting column immediately before use. The measurement of the heme Soret peak at 422 nm verified successful removal of the dithiothreitol (DTT) present in the storage buffer.

- (15) Siddhanta, U.; Wu, C.; Abu-Soud, H. M.; Zhang, J.; Ghosh, D. K.; Stuehr, D. J. *J. Biol. Chem.* **1996**, *271*, 7309–7312.
- (16) Kobayashi, K.; Tagawa, S.; Daff, S.; Sagami, I.; Shimizu, T. *J. Biol. Chem.* **2001**, *276*, 39864–39871.
- (17) Panda, K.; Ghosh, S.; Stuehr, D. J. *J. Biol. Chem.* **2001**, *276*, 23349–23356.
- (18) Abu-Soud, H. M.; Yoho, L. L.; Stuehr, D. J. *J. Biol. Chem.* **1994**, *269*, 32047–32050.
- (19) Crane, B. R.; Arvai, A. S.; Gachhui, R.; Wu, C.; Ghosh, D. K.; Getzoff, E. D.; Stuehr, D. J.; Tainer, J. A. *Science* **1997**, *278*, 425–431.
- (20) Raman, C. S.; Li, H.; Martasek, P.; Kral, V.; Masters, B. S. S.; Poulos, T. L. *Cell* **1998**, *95*, 939–950.
- (21) Poulos, T. L.; Li, H.; Raman, C. S.; Schuller, D. J. *Adv. Inorg. Chem.* **2001**, *51*, 243–293.
- (22) Dmochowski, I. J.; Crane, B. R.; Wilker, J. J.; Winkler, J. R.; Gray, H. B. *Proc. Natl. Acad. Sci. U.S.A.* **1999**, *96*, 12987–12990.
- (23) Wilker, J. J.; Dmochowski, I. J.; Dawson, J. H.; Winkler, J. R.; Gray, H. B. *Angew. Chem., Int. Ed.* **1999**, *38*, 90–92.
- (24) Dmochowski, I. J.; Dunn, A. R.; Wilker, J. J.; Crane, B. R.; Green, M. T.; Dawson, J. H.; Sligar, S. G.; Winkler, J. R.; Gray, H. B. *Methods Enzymol.* **2002**, *357*, 120–133.
- (25) Low, D. W.; Winkler, J. R.; Gray, H. B. *J. Am. Chem. Soc.* **1996**, *118*, 117–120.
- (26) Berglund, J.; Pascher, T.; Winkler, J. R.; Gray, H. B. *J. Am. Chem. Soc.* **1997**, *119*, 2464–2469.
- (27) Dunn, A. R.; Dmochowski, I. J.; Winkler, J. R.; Gray, H. B. *J. Am. Chem. Soc.* **2003**, *125*, 12450–12456.
- (28) Dunn, A. R.; Dmochowski, I. J.; Bilwes, A. M.; Gray, H. B.; Crane, B. R. *Proc. Natl. Acad. Sci. U.S.A.* **2001**, *98*, 12420–12425.
- (29) (a) Dunn, A. R.; Hays, A. M. A.; Goodin, D. B.; Stout, C. D.; Chiu, R.; Winkler, J. R.; Gray, H. B. *J. Am. Chem. Soc.* **2002**, *124*, 10254–10255. (b) Hays, A. M. A.; Dunn, A. R.; Chiu, R.; Gray, H. B.; Stout, C. D.; Goodin, D. B. *J. Mol. Biol.* **2004**, *344*, 455–469.
- (30) Ortiz de Montellano, P. R. *Cytochrome P450: Structure, Mechanism, and Biochemistry*; Plenum Press: New York, 1995.
- (31) Ghosh, D. K.; Wu, C.; Pitters, E.; Moloney, M.; Werner, E. R.; Mayer, B.; Stuehr, D. J. *Biochemistry* **1997**, *36*, 10609–10619.

High-spin, dimeric $\Delta 65$ iNOS was generated by incubating $\Delta 65$ with 1 mM tetrahydrobiopterin (H_4B) and 1 mM arginine (Arg) for 2 h at 4 °C before diluting the sample to final concentrations of 0.1 mM H_4B and 1 mM Arg. Satisfactory Arg and H_4B binding was signaled by a shift of the Soret to 396 nm. NOS extinction coefficients were determined using the hemochromogen assay; 1 mL of NOS solution was diluted with 0.125 mL of 0.5 M NaOH and 0.125 mL of pyridine, and then reduced with several grains of sodium dithionite. The resulting ferrohemochromogen concentration was calculated using an extinction coefficient of 31 mM^{−1} cm^{−1} at 556 nm. The assays were calibrated using cytochrome P450cam ($\epsilon_{416} = 115$ mM^{−1} cm^{−1}).³² The NOS extinction coefficients calculated using this method are substrate-free $\Delta 65$ (− H_4B , −Arg) $\epsilon_{422} = 75$ mM^{−1} cm^{−1}, $\Delta 65$ (+ H_4B , +Arg) $\epsilon_{396} = 75$ mM^{−1} cm^{−1}, and substrate-free $\Delta 114$ $\epsilon_{422} = 85$ mM^{−1} cm^{−1}.

Ru–wires (**1–3**) were prepared by the literature procedure.²⁷ The fluorinated biphenyl bridging moieties for Re–wires **4** and **5** were synthesized by reacting imidazole and perfluorobiphenyl in dimethyl sulfoxide. The resulting mono- and disubstituted perfluorobiphenyl–imidazole ligands were separated by flash silica chromatography. Re-(dimethylphenanthroline)(CO)₃Cl was treated with silver triflate, and then reacted with either the mono- or disubstituted perfluorobiphenyl–imidazole ligand to form **4** and **5** as triflate salts.³³

Both time-resolved and steady-state spectroscopic measurements were performed as previously described.²⁷ Luminescence decay profiles were fit to a biexponential function (eq 1):

$$I(t) = c_1 e^{-k_1 t} + c_2 e^{-k_2 t} \quad (1)$$

using a nonlinear least-squares algorithm. The ratio of enzyme-bound to free ruthenium complex is $c_1:c_2$, where k_1 and k_2 are the luminescence decay rate constants for the enzyme-bound and free ruthenium complexes. Dissociation constants were derived from $c_1:c_2$ as previously described.²⁷

Characteristic FET distances (R_0) for the Ru– and Re–diimine wires with iNOSoxy were calculated from the probe emission and NOS absorption spectra.²⁷ These distances are 24.3 Å for **1** and **2** with $\Delta 114$, 19.6 Å for **3** with $\Delta 114$, 32 Å for **4** and **5** with $\Delta 114$, 24.3 Å for **1** and **2** with substrate-free $\Delta 65$, 19.5 Å for **3** with substrate-free $\Delta 65$, 23.9 Å for **1** and **2** with Arg- and H_4B -bound $\Delta 65$, and 19.3 Å for **3** with Arg- and H_4B -bound $\Delta 65$.

Results and Discussion

Ru–Wires. Two murine iNOSoxy truncation mutants, $\Delta 114$ and $\Delta 65$, were investigated. Importantly, $\Delta 114$ is predominantly monomeric, while $\Delta 65$ exists in a monomer–dimer equilibrium, forming a strong dimer in the presence of H_4B .³¹ For clarity, both $\Delta 65$ without bound H_4B and $\Delta 114$ are referred to below as “monomeric”. Monomeric iNOSoxy has an exposed active site (see below), while dimeric iNOSoxy has a much more constricted substrate access channel.

No change in the iNOSoxy heme absorption spectrum was observed upon stoichiometric addition of **1** or **3** to either $\Delta 114$ or $\Delta 65$. In contrast, the addition of excess **2** to $\Delta 114$ or monomeric $\Delta 65$ (− H_4B , −Arg) resulted in a heme Soret shift from 420 to 422 to 426 nm, consistent with imidazole ligation of the heme (Figure 1). The absorption spectrum of dimeric $\Delta 65$ (+ H_4B , +Arg) was not altered in the presence of **1–3**, indicating that none of the Ru–wires displaces Arg from the dimeric iNOSoxy active site.

In all cases, biexponential Ru–wire luminescence decays were observed in the presence of stoichiometric $\Delta 114$ or $\Delta 65$,

(32) Sligar, S. G. *Biochemistry* **1976**, *15*, 5399–5406.

(33) Belliston-Bittner, W.; Dunn, A. R.; Winkler, J. R.; Getzoff, E. D.; Stuehr, D. J.; Gray, H. B. Manuscript in preparation.

Table 1. Ru–Wire Dissociation Constants and Ru–Fe Distances from FET Kinetics^a

compound	$\Delta 114$		$\Delta 65$		$\Delta 65 + \text{Arg, } +\text{H}_4\text{B}$	
	K_d (μM)	Ru–Fe (\AA)	K_d (μM)	Ru–Fe (\AA)	K_d (μM)	Ru–Fe (\AA)
1	0.88 ± 0.15	18.9 ± 0.1	0.54 ± 0.04	19.6 ± 0.2	1.7 ± 0.4	19.6 ± 0.4
2	7.1 ± 0.4	17.8 ± 0.5	6.5 ± 2.4	19.3 ± 0.6	7.2 ± 3.4	20.9 ± 0.8
3	0.71 ± 0.09	20.1 ± 0.1	0.58 ± 0.16	20.2 ± 0.4	0.89 ± 0.15	21.0 ± 0.3

^a Uncertainties are the root-mean-square deviations calculated from independent measurements (3 for $\Delta 114$, 2 for $\Delta 65$, 3 for $\Delta 65 + \text{H}_4\text{B}$, +Arg).

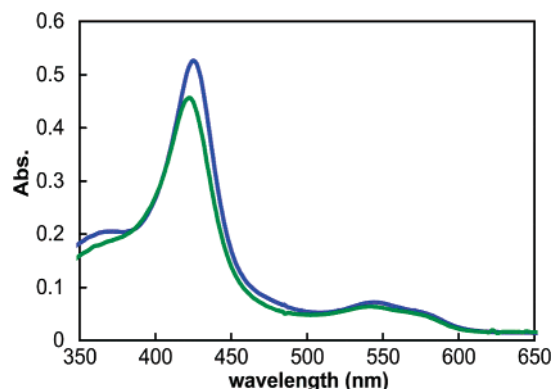


Figure 1. UV–visible absorption spectrum of $\Delta 114$ alone ($5.7 \mu\text{M}$; green) and bound to **2**, corrected for the absorption attributable to the Ru–wire ($+20.5 \mu\text{M}$ **2**; blue).

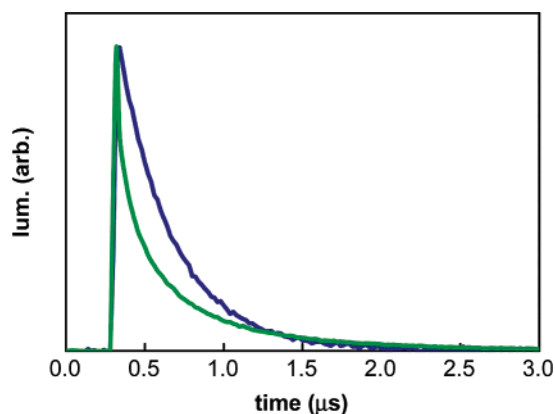


Figure 2. Sample transient luminescence decay data for **1** (blue) and a 1:1 mixture of **1** and $\Delta 65$ ($1.8 \mu\text{M}$; green). The fast component of the luminescence decay corresponds to **1** bound to $\Delta 65$.

indicating that the Ru–wires bind to the enzyme (Figure 2). Quenching of the Ru–wire excited state could, in principle, occur by either energy or electron transfer to the iNOSoxy heme. Since no electron-transfer products were observed by transient UV–visible absorption spectroscopy, and because the rate of luminescence quenching is consistent with FET, energy transfer is the probable mechanism of Ru–wire luminescence quenching. The weightings of the fast and slow luminescence decay phases were used to calculate dissociation constants, while the rates of energy transfer were used to calculate Ru to heme–Fe distances. Ru–Fe distances so obtained for Ru–wire:P450cam conjugates matched those observed in the corresponding crystal structures to within 0.4 \AA .²²

The Ru–wires bind with micromolar dissociation constants and with Ru–Fe distances of $18\text{--}21 \text{ \AA}$ (Table 1). Interestingly, **1** and **3** bind $\Delta 114$, $\Delta 65$, and dimeric $\Delta 65$ ($+\text{H}_4\text{B}$, +Arg) with dissociation constants that are virtually identical. The Ru–Fe distances calculated for **1** and **3** are similar for $\Delta 114$ and $\Delta 65$ and are unaffected by the presence of H_4B and Arg (Table 1).

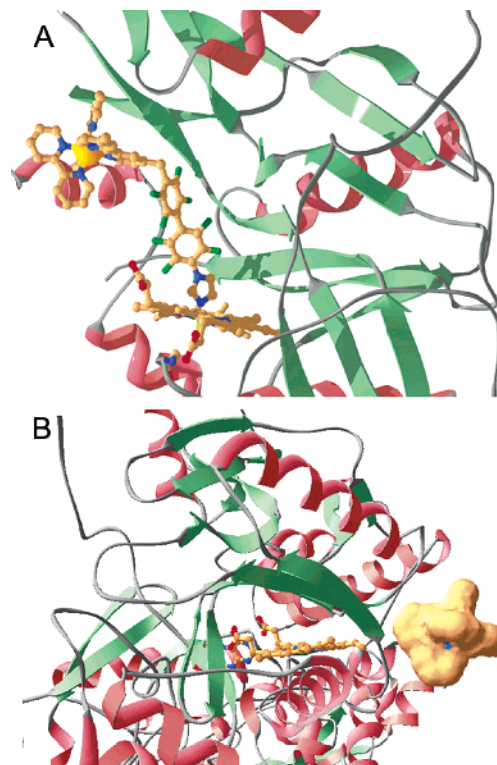


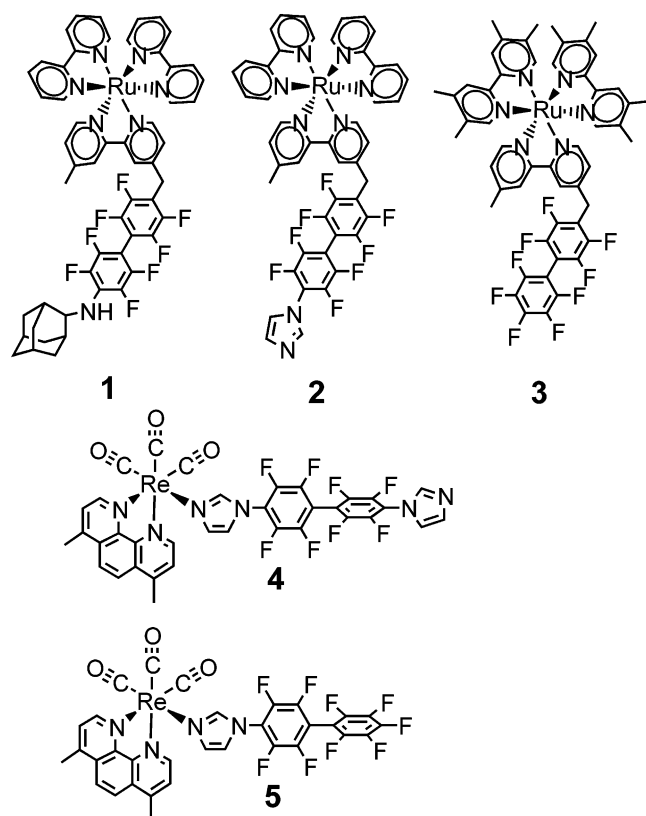
Figure 3. (A) Model of **2** bound to the exposed heme of monomeric $\Delta 114$. The Ru–Fe distance in this model is 16.9 \AA . (B) The NOS dimer, shown with $\text{Ru}(\text{bpy})_3$ (van der Waals surface) docked at the proposed reductase binding site. The Ru–Fe distance is $\sim 19 \text{ \AA}$, consistent with the Ru–Fe distances measured for the $\Delta 65:1$ and $\Delta 65:3$ conjugates.

The spectroscopic evidence suggests that **1** and **3** do not bind in the active site; the heme absorption spectrum is not altered in the presence of **1** or **3**, and the K_d values and Ru–Fe distances determined for these Ru–wires are not substantially altered by the addition of H_4B and Arg. Addition of stoichiometric **4**, which binds in the iNOS active site (see below), does not alter the binding of **3** to monomeric $\Delta 65$, again demonstrating that **3** does not bind in the active site (Supporting Information).

Consistent with these data, modeling suggests that **1** and **3** cannot fit into the substrate access channel of dimeric $\Delta 65$ ($+\text{H}_4\text{B}$, +Arg), owing to the bulk of the ruthenium tris-bipyridyl moiety. Instead, the calculated Ru–Fe distances indicate that **1** and **3** may bind on the distal side of the enzyme, at the proposed binding site of the reductase module (Figure 3b).¹⁴ The proposed binding site is concave and hydrophobic. The Ru–wires present few opportunities for specific interactions with the protein surface. Instead, extensive wire:protein hydrophobic contacts likely mediate binding. Of interest in this regard is that other Ru^{II} –diimines bind cytochrome *c* oxidase at the physiologically relevant cytochrome *c* binding site.^{34,35}

(34) Zaslavsky, D.; Sadoski, R. C.; Wang, K. F.; Durham, B.; Gennis, R. B.; Millett, F. *Biochemistry* **1998**, *37*, 14910–14916.

Chart 1. Ru–Wires (**1–3**) and Re–Wires (**4** and **5**) Bind iNOSoxy and also Cytochrome P450cam



In contrast, the shifts in the absorption spectra of monomeric $\Delta 65$ and $\Delta 114$ in the presence of excess **2** clearly indicate that the imidazole of **2** ligates the heme (Figures 1 and 3a).¹⁹ Structural modeling suggests that the less bulky **2**, which lacks the adamantyl group of **1** and the tetramethylbipyridine ligands of **3**, can bind in the more exposed active site of monomeric iNOSoxy (Figure 3a). However, **2** may also bind iNOSoxy at the site occupied by **1** and **3**; 1.5 equivalents of **2** bind to monomeric $\Delta 65$ (–H₄B, –Arg) when the Ru–wire is present in 6-fold excess, and **2** binds to dimeric $\Delta 65$ (+H₄B, +Arg), in which the active site is occupied. In contrast to those in **1** and **3**, the Ru–Fe distances determined for the **2**: $\Delta 114$ and **2**: $\Delta 65$ +H₄B, +Arg conjugates increase markedly from 17.8 to 20.9 Å, suggesting a different mode of binding to monomeric ($\Delta 114$) and dimeric ($\Delta 65$ +H₄B, +Arg) iNOSoxy. These data together suggest that **2** binds to both the active site of monomeric iNOSoxy and another portion of the protein with similar *K_d* values.

Re–Wires. Luminescent rhenium diimines, [Re(CO)₃(L₂)-(L₂')]⁺, where L₂ is a 2,2'-bipyridyl or phenanthryl derivative, and L₂' is a nitrogen donor, such as imidazole or pyridine, typically have microsecond excited-state lifetimes. Like Ru-(bpy)₃²⁺, the excited states are both good oxidants (~1.2 V vs NHE) and reductants (–0.7 V vs NHE).³⁶ In addition, photochemically generated [Re(CO)₃(L₂)(L₂')]²⁺ complexes are extremely strong oxidants (~1.8 V vs SCE).³⁷

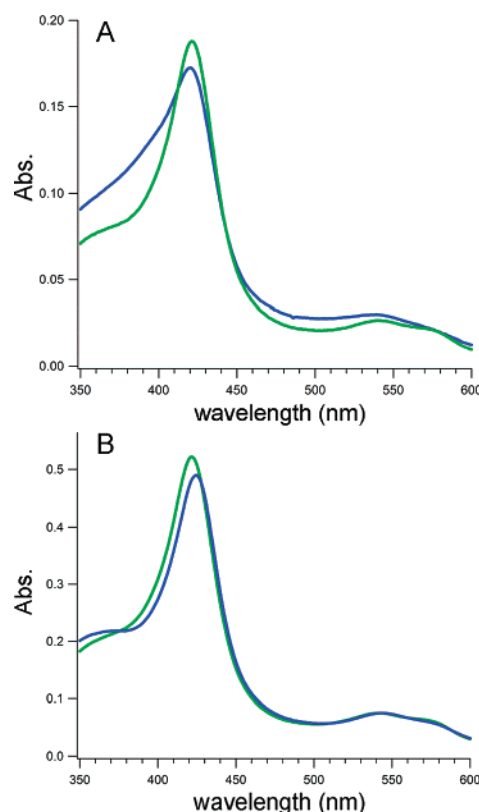


Figure 4. (A) 2.2 μ M $\Delta 114$ alone (green) and with stoichiometric **5** (blue). Both the slight shift in peak wavelength and development of a pronounced shoulder indicate partial conversion to high-spin, five-coordinate heme. (B) 6.0 μ M $\Delta 114$ alone (green) and with stoichiometric **4** (blue). The red shift in peak wavelength is consistent with imidazole ligation of the heme.

To take advantage of rhenium photochemistry, we synthesized Re–wires **4** and **5** (Chart 1). The complexes are structurally similar to **1** and **3**, but the Re–photosensitizer is smaller. The surface areas of [Ru(bpy)₃]²⁺ and [Re(CO)₃(dimethylphenanthroline)(imidazole)]⁺ are 650 and 550 Å², respectively.³⁸ Additionally, the *fac*-carbonyls of **4** and **5** result in a more compact profile on one side of the complex, allowing a closer approach to the protein. The virtually identical absorption spectra of **4** and **5** are typical of Re–diimines. Both complexes are luminescent, with emission spectra centered at 560 nm (quantum yields are 0.055 in phosphate buffer).

Upon addition of **4** to $\Delta 114$ murine iNOSoxy, the Soret shifts from 422 to 426 nm, signaling imidazole ligation to the heme iron (Figure 4b). Time-resolved luminescence measurements indicate that **4** is almost completely bound to NOS in 1:1 micromolar solutions (data not shown). Indeed, a *K_d* could not be determined from the luminescence decay data due to the rapidity of the decay³⁹ and the almost complete absence of a slow decay rate corresponding to free **4** in solution. Instead, a dissociation constant of 100 ± 80 nM was calculated from a comparison of the steady-state luminescence spectra of **4** alone and bound to $\Delta 114$ iNOSoxy (Figure 5).

Re–wire **5** causes a blue shift in the $\Delta 114$ Soret, indicating partial conversion to a high-spin, five-coordinate heme (Figure 4a). In addition to a small shift in peak wavelength, a noticeable shoulder appears in the Soret (Figure 4a), consistent with partial

(35) Zaslavsky, D.; Kaulen, A. D.; Smirnova, I. A.; Vygodina, T.; Konstantinov, A. A. *FEBS Lett.* **1993**, 336, 389–393.

(36) Connick, W. B.; DiBilio, A. J.; Hill, M. G.; Winkler, J. R.; Gray, H. B. *Inorg. Chim. Acta* **1995**, 240, 169–173.

(37) Sacksteder, L.; Zipp, A. P.; Brown, E. A.; Streich, J.; Demas, J. N.; Degraff, B. A. *Inorg. Chem.* **1990**, 29, 4335–4340.

(38) Gerstein, M. *Acta Crystallogr. A* **1992**, 48, 271–276.

(39) Initial data suggest that the luminescence quenching is attributable to rapid electron transfer (ref 33).

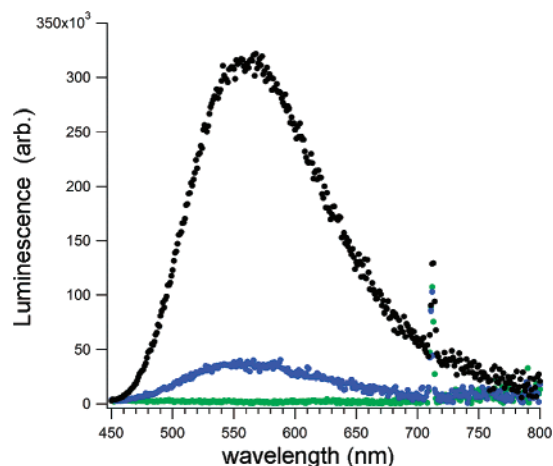


Figure 5. Steady-state luminescence spectra of 2.6 μM samples of $\Delta 114$ (green), **4** (black), and a 1:1 mixture of $\Delta 114$ and **4** (blue). The luminescence of **4** is strongly quenched in the presence of $\Delta 114$, making it a sensitive indicator of the presence of the enzyme. The sharp spike at 710 nm is an artifact arising from scattered 355-nm excitation light.

displacement of the iron-ligating water from the active site. The time-resolved luminescence decay spectra (Supporting Information) suggest that **5** binds with a dissociation constant of $5 \pm 2 \mu\text{M}$ and a Re-heme distance of $\sim 18 \text{ \AA}$. Both the changes in the Soret absorption and the calculated Re-Fe distance are consistent with **5** binding in the active site. Structural modeling indicates that **5** can fit in the active site of monomeric iNOSoxy, unlike the sterically bulkier **3**. The structural dissimilarities of **5** and Arg make it surprising that **5** binds at all. However, the relatively exposed active site of the monomeric $\Delta 114$ iNOSoxy provides good surface complementarity with the fluorinated biphenyl moiety.

Concluding Remarks

Small molecules that interfere with NOS function are being investigated as potential treatments for several diseases.^{40,41} All currently known inhibitors in this class bind in the active site of the enzyme. In contrast, Ru-wires or similar compounds may provide an effective means of NOS inhibition by preventing

electron transfer between the reductase module and oxygenase domain. Inhibitors that disrupt protein:protein interactions could be of great value, owing to the biological ubiquity of transient protein complexes.

The interactions of **2** and **4** with $\Delta 114$ are in many ways analogous to those observed with small molecules that prevent NOS holoenzyme dimerization.⁴² Because only iNOS exhibits an appreciable monomer-dimer equilibrium in vivo, these inhibitors are highly isoform selective.⁴² The low dissociation constant of **4** makes it a useful lead compound for further development. The ~ 70 -fold difference in dissociation constants between **2** and **4** illustrates the steric influence of the $\text{Ru}(\text{bpy})_3^{2+}$ moiety.

The ability of **5** to bind in or near the iNOSoxy active site is remarkable given its dissimilarity to Arg or known inhibitors. As with the Ru-wires, it seems likely that binding is driven principally by hydrophobic interactions. Although **3** binds more tightly than **5** to NOS, it does not produce a similar shift in the absorption spectrum, again demonstrating the importance of steric bulk in modulating wire-NOS interactions.

Most notably, we have shown the usefulness of FET kinetics in characterizing small molecule:protein interactions. Conventional UV-visible absorption measurements or competition binding assays would have overlooked the ability of **1** and **3** to bind iNOSoxy. What is more, FET measurements yield distance constraints, which provide additional information about the interaction between the wire and target enzyme. As demonstrated by these results, FET data greatly facilitate the formulation of structural models for wire:enzyme conjugates.

Acknowledgment. We thank John Magyar for helpful discussions. This work was supported by the Fannie and John Hertz Foundation (A.R.D.), the National Institutes of Health (W.B., E.D.G.), and the National Science Foundation (H.B.G., J.R.W.).

Supporting Information Available: Further transient luminescence decay kinetics. This material is available free of charge via the Internet at <http://pubs.acs.org>.

JA046971M

(40) Salerno, L.; Sorrenti, V.; Di Giacomo, C.; Romeo, G.; Siracusa, M. A. *Curr. Pharm. Des.* **2002**, *8*, 177–200.

(41) Vallance, P.; Leiper, J. *Nat. Rev. Drug Discovery* **2002**, *1*, 939–950.

(42) McMillan, K.; Adler, M.; Auld, D. S.; Baldwin, J. J.; Blasko, E.; Browne, L. J.; Chelsky, D.; Davey, D.; Dolle, R. E.; Eagen, K. A.; Erickson, S.; Feldman, R. I.; Glaser, C. B.; Mallari, C.; Morrissey, M. M.; Ohlmeyer, M. H. J.; Pan, C. H.; Parkinson, J. F.; Phillips, G. B.; Polokoff, M. A.; Sigal, N. H.; Vergona, R.; Whitlow, M.; Young, T. A.; Devlin, J. J. *Proc. Natl. Acad. Sci. U.S.A.* **2000**, *97*, 1506–1511.